Journal of Geomatics Vol 9 No. 1 April 2015

Feature extraction of hyperspectral imaging data using texture analysis

Rimjhim Bhatnagar Singh[1], S.S. Ray[2] and A.C. Sharma[3]

[1]Space Applications Centre, ISRO, Ahmedabad-15, India
[2]Mahalanobis National Crop Forecast Centre, Pusa Campus, New Delhi-12, India
[3] MS University, Baroda, India
Email: rimjhim@sac.isro.gov.in

(Received: Sep 17, 2014; in final form: Feb 04, 2015)

Abstract: Hyperspectral remote sensing is a tool for identifying objects using their spectral signatures based on the principles of imaging spectroscopy. But, a very large number of bands available in hyperspectral data pose serious problems in computation speed as well as may produce erroneous results due to data redundancy. This drawback demands feature reduction/extraction of hyperspectral data specific to the purpose, which in this case is vegetation discrimination. This work highlights technique of feature extraction based on image texture for Hyperion data over a controlled forest site. A total of six texture measures were analyzed for feature extraction and best among them are reported in this paper. The technique was compared with conventionally used Minimum Noise Fraction (MNF) technique by evaluating its performance for classification of forest species. A number of other classifiers were also evaluated. Comparison of classification results with the ground data yielded an accuracy of 82.73% with the proposed method of feature extraction and Support Vector Machine (SVM) as classifier while 65% accuracy in case of conventionally used method of MNF coupled with parallelpiped classifier.

Keywords: Hyperspectral feature extraction, Image texture, MNF, Classification

1. Introduction

Broadband remote sensing data had been widely used for various land applications in the yonder years. However, in order to enhance the application of remote sensing data in various applications, the era of hyperspectral remote sensing has emerged in the recent past. Hyperspectral sensors acquire reflectance values at hundreds of different wavelengths thereby enabling detailed applications in the field of agriculture, mineral exploration etc (e.g. Goetz, 2009; Champagne et al., 2001; Clark et al., 1990). Large numbers of narrowly spaced bands often exhibit high correlation between them leading to undesirable band redundancy, which hinders correct and accurate hyperspectral image analysis. Therefore, dimensionality extraction, within the trade-off constraint of error and speed, is absolutely necessary for useful applications.

Supervised classification requires n^2-1 training sites (Hughes, 1968), where n is the number of bands. For broadband data, this condition is easily met, but, with hundreds of bands, hyperspectral data poses serious limitations on selection of training sites (Hughes Phenomenon, Richards and Jia, 2006), classifier adopted and hence degrades classification accuracy. Much work has been carried out in the past to overcome this issue. Various techniques have thus evolved in the past which include distance measures like Bhattacharya distance and JM distance (Richards and Jia, 2006), divergence and transformed divergence techniques; eigen value approaches like Principal Component Analysis (Farrell and Mersereau, 2005) and Minimum Noise fraction (Boardman and Kruse, 1994) etc. Divergence methods are more suitable for multi-spectral data. When they are applied to hyperspectral imagery, the calculations become enormous and, hence, difficult. PCA neither computes noise statistics nor optimizes SNR but only reorders the transformed components in terms of decreasing image quality, which may not be always true (Green et al., 1988). MNF requires a priori knowledge of noise and non-singular matrices for computation of covariance. Another weakness of MNF lies in its shift difference approach, which requires a homogeneous patch having pixel number greater than number of bands. This implies that determination of suitable dimensionality extraction method for a particular application is a tough job.

Images, generally, contain regions characterized by variations in brightness instead of unique brightness values. Image texture refers to such spatial variations in image tone. It is a storehouse of information through which quantification of the perceived texture of an image can be done, thereby, describing the spatial arrangement of pixel intensities in an image (Shapiro and George, 2001). Texture analysis has tremendous applications in many areas including remote sensing applications. Although, in the field of medical imaging, texture analysis has demonstrated its crucial role, however, it is in the state of budding development for remote sensing applications. Image texture can be defined in terms of various parameters like image entropy, homogeneity etc which show independent aspects of the images. Hence, in this work, image texture has been utilized to reduce data dimensionality with the objective of classification of tree species.

Conventionally used dimensionality reduction technique MNF was also used in this study, particularly for comparing with the techniques mentioned above. Besides feature extraction, selection of suitable classification technique for hyperspectral images is equally important. While attempting supervised classification of hyperspectral data, the small ratio between the number of available training samples and the number of features (Hughes effect, Hughes (1968)) pose serious difficulty in the process. Consequently, the standard classifiers used for multi-spectral data are not suitable. Techniques specific to hyperspectral data like Spectral Angle Mapper (SAM) are the substitute. However, if features are appropriately selected/extracted, the richness of other classifiers can also be explored. In this paper, various classification techniques are investigated by using two types of dimensionality reduction/ extraction methods.

2. Study area

The study was carried out for the tree species present in the experimental plots of Forest Research Institute, Dehradun, Uttarakhand, India. The lush green estate spreads over 450 ha, with the outer Himalayas forming its backdrop. The topography of the area is of gentle relief, with elevation ranging from 584 to 617 m above sea level. The area is a typical representative of some of the country's major forest species i.e. Chir pine (Pinus roxbhurghii), Tropical Pine (Pinus caribea), Teak (Tectona grandis), Sal (Shorea robusta), Saza (Terminalia tomentosa) and Eucalyptus (Eucalyptus hybrid).

3. Materials and methods

3.1 Data used

Data from space borne push-broom sensor Hyperion, onboard NASA's EO-1 satellite having 242 bands in 400nm-2500nm range of electromagnetic spectrum and at an average resolution of 10nm was used for this study. The data selected was of level 1Gst, dated 25th December 2006. Level 1Gst is radiometrically corrected and orthorectified data. Table 1 lists some of the important characteristics of the sensor.

Table 1: Hyperion specifications (Pearlman et al., 2001)

Number of bands	242 (196 calibrated and unique bands)
Spectral range (μm)	0.4-2.5
Spatial resolution	30m
Radiometric Accuracy	6%
Swath	7.5 km
GSD	30m
Quantization	12 bit
Orbit height	705 km

3.2 Data pre-processing

Hyperion data consists of 242 bands including 44 uncalibrated bands (1–7, 58-76, 225–242). Besides this, bands 56–57 and 77–78 are overlapping. Hence, on removing the uncalibrated and overlapping bands, a total of 196 unique spectral channels were obtained. A spatial subset of the Hyperion scene was extracted for the study. The level 1Gst Hyperion data is inherently georeferenced and radiometrically corrected. Hence, only atmospheric correction was done as the preliminary step. Atmospheric correction involves selection of suitable aerosol and atmospheric model, water and aerosol retrieval. This process was performed using the atmospheric correction module Fast Line-of-sight Atmospheric Analysis of Spectral Hypercubes (FLAASH) of ENVI image processing software which corrects wavelengths from 0.0004 mm approximately to up to 3 mm. The reason for using FLAASH over other methods is because it incorporates the MODTRAN4 radiation transfer code, as a result, it quite accurately compensates for atmospheric effects (Matthew et al., 2000).

3.3 Feature extraction

3.3.1 Image texture based feature extraction: Two basic categories of texture analysis can be defined, namely, statistical and structural. Statistical texture analysis techniques primarily describe texture of regions in an image through higher-order moments of their grayscale histograms (Tomita and Tsuji, 1990). In simpler terms, it can be said that statistical approach sees an image texture as a quantitative measure of the arrangement of intensities in a region. On the other hand, structural texture analysis techniques describe texture as to comprise of well-defined texture elements. Texture analysis based on extracting various textural features from a gray level co-occurrence matrix (GLCM) (Haralick et al., 1973) is the most popular and cited technique. The GLCM approach is based on the use of second-order statistics of the grayscale image histograms. The GLCM functions characterize the texture of an image by calculating the co-occurrences of pixels with specific values in an image, creating a GLCM, and then extracting statistical measures from this matrix. The GLCM of an image is an estimate of the second-order joint probability, $P_\delta(i,j)$ of the intensity values of two pixels (i and j), a distance δ apart along a given direction. Haralick et al. (1973) proposed 14 textural parameters calculated from $\mathbf{P}_\delta$, all of which are seldom used. However, the correct choice of parameters lies in their ability to extract the most prominent features. For example, in areas with smooth texture, the range of values in the neighborhood around a pixel will be a small value; in areas of rough texture, the range will be larger. Similarly, calculating the standard deviation of pixels in a neighborhood can indicate the degree of variability of pixel values in that region. Therefore, GLCM based texture analysis was employed for this work. This method includes 'variance', 'homogeneity' (Measures closeness of elements in GLCM to the diagonal elements), 'contrast' (Measures local variations), 'dissimilarity', 'correlation' (Measures joint probability) and 'entropy' (Degree of randomness) of the image in order to assess the suitable bands for discrimination purpose. Table 2 describes methods of computation for the said texture measures. In addition, the table gives computation methods for 'mean' and 'standard deviation'.

Journal of Geomatics Vol 9 No. 1 April 2015

Table 2: Computation formulae for texture measure

Texture measure	Method of computation
Entropy	$S= -\Sigma_{i=1 \text{ to } n} \Sigma_{j=1 \text{ to } n} P_\delta (i,j) \log P_\delta (i,j)$
Contrast	$C=\Sigma_{k=0 \text{ to } n-1} k^2\Sigma_{i=1 \text{ to } n} \Sigma_{j=1 \text{ to } n} P_\delta (i,j)$
Correlation	$Co= (\Sigma_{i=1 \text{ to } n} \Sigma_{j=1 \text{ to } n} i.j\ P_\delta (i,j)-\mu_x\mu_y)/\sigma_x\sigma_y$
Homogeneity	$H= \Sigma_{i=1 \text{ to } n} \Sigma_{j=1 \text{ to } n} P_\delta (i,j)/(1+\|i-j\|)$
Mean	$\mu_x= \Sigma_{i=1 \text{ to } n} \Sigma_{j=1 \text{ to } n} P_\delta (i,j)$ $\mu_y =\Sigma_{j=1 \text{ to } n} \Sigma_{i=1 \text{ to } n} P_\delta (i,j)$
Standard Deviation	$\sigma_x= \Sigma_{i=1 \text{ to } n} (i-\mu_x)^2 \Sigma_{j=1 \text{ to } n} P_\delta (i,j)$ $\sigma_y= \Sigma_{j=1 \text{ to } n} (j-\mu_y)^2 \Sigma_{i=1 \text{ to } n} P_\delta (i,j)$
Variance	$(\sigma)^2$

3.3.2 Minimum Noise Fraction (MNF) based feature extraction: Principal components analysis (PCA) is a popular technique for data compression that produces uncorrelated bands, segregates noise and reduces dimensionality (Richards, 1999). It transforms data coordinates in a manner such that the first principal component is along the direction of maximum variance. It then maximizes the variance in successive components. However, Farrell and Mersereau (2005) suggested that for targeting at activities like discrimination of objects, PCA is not suitable. Nonetheless, Minimum Noise Fraction (MNF) transform, which essentially is noise adjusted PCA, is a better alternative. It is a two stage linear transform where noise is decorrelated and rescaled followed by PCA (Green et al., 1988). Hence, out of the conventionally used eigen value based techniques of feature extraction, MNF was adopted for this study mainly to compare with the proposed technique.

3.4 Classification

The features bearing uniqueness and rich in information content generated by coagulating the dominant characteristics of the target are the most useful ones. Simultaneously, the choice of classifier also plays a great role in proper species discrimination. Hence, the dimensions obtained by using the two techniques were evaluated by comparing the classification results obtained from the use of various classifiers. Apart from the conventionally used maximum likelihood, minimum distance, Mahalanobis and parallelepiped classifiers, the comparatively newer techniques like Support Vector Machine (SVM), Spectral Angle Mapper (SAM), Neural Network and Binary Encoding were also evaluated. SVM separates the classes with a decision surface, called hyperplane that maximizes the margin between the classes. The data points closest to the hyperplane are called support vectors and are crucial for training sets. It often gives good classification results for noisy datasets. SAM is a classifier that uses an n-dimensional angle to match pixels to reference spectra by calculating the angle between the spectra by treating them as vectors in a space with dimensionality equal to the number of bands (Kruse et al., 1993). Binary encoding encodes the data and spectra into binary numbers, based on bands falling below or above the spectrum mean, respectively. An XOR function compares each encoded reference spectrum with the encoded data spectra and produces a classification image (Mazer et al., 1988).

4. Results and discussions

4.1 Image texture based feature extraction and classification

In order to select the suitable bands for vegetation discrimination, the texture measures, variance, homogeneity, contrast, dissimilarity, correlation and entropy were computed using GLCM. The GLCM matrix was created using each pixel along with its immediate horizontal neighbor (x shift=1 and y shift=0) for a 3*3 pixel window. Each texture measure owned 196 images. Good quality bands (SNR>10) were selected for each texture measure. This reduced the number of bands corresponding to each parameter. Finally, intersection of sets of bands was done to yield final number of reduced bands available for further analysis. Table 3 shows the permissible values for different texture measures corresponding to SNR>10, below which the bands were removed. SNR computation was done by selecting 3*3 pixel window from the scene for which average DN and standard deviation (S.D.) were computed. SNR was thus calculated as (Schowengerdt, 1997):

$$SNR=\text{mean DN}/ S.D. \qquad (1)$$

Outside the permissible values, the bands extracted played insignificant to poor roles in image classification either by not affecting classification accuracy at all or by decreasing it by a few percentages. Also, each texture measure was analyzed for its significance in modulating classification accuracy. This was done by deliberately removing one texture measure at a time in the analysis to check the effect it imparts to the classification accuracy. Because, no significant contribution was shown by the parameters homogeneity and correlation in feature extraction by observing classification results, consequently, the same were dropped from further analysis.

Table 3: Texture measures

S. No.	Texture measure	Permissible value
1	Variance	>30
2	Homogeneity	Not suitable
3	Contrast	<10
4	Dissimilarity	>4
5	Entropy	>1
6	Correlation	Not suitable

The above-mentioned criteria reduced the number of bands. However, the different texture measures ended up with different sets of bands. Hence, intersection of sets was performed to select the bands common to all parameters. Accordingly, out of 196 unique bands, best 56 bands were selected of which 22 fell in the range 427-630nm (Chlorophyll absorption region), 1 band centered at 681nm (also a Chlorophyll absorption region), 2 bands within 1073-1083nm, 7 bands between 1114 - 1185nm, 21 within 1457-1659nm (Lignin, cellulose and nitrogen absorption regions) and 3 within 1861-1901nm. These bands were then adopted for further analysis i.e. classification. It is noteworthy that dominant absorption features are automatically selected through this procedure. Figure 1 shows the bands selected as a consequence of image texture analysis. It may be noted that frequency value 4 shows the common bands obtained through all the texture measures collectively and hence the corresponding bands were selected.

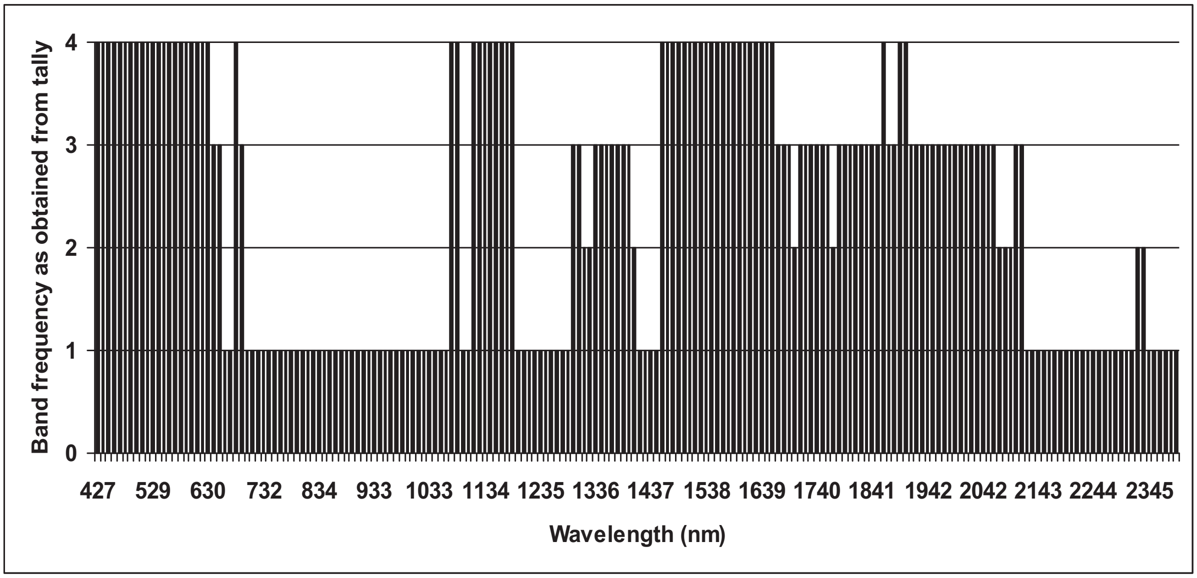

Figure 1: Bands selected after intersection of sets of bands corresponding to different texture measures

Forward MNF transform yielded a large number of bands but with constraint of eigen value > 10 along with the simultaneous check on image noise, 6 MNF bands were obtained. These were the bands that were used for discrimination purpose.

Although, a large number of classifiers are available, yet, a careful selection of classifier is required for optimal result having close resemblance with the ground conditions. Supervised classification was performed by using the ground truth map of the study area. Various classifiers were evaluated for different dimensionality reduction techniques. Confusion matrices were generated post classification. Table 4 shows a detailed comparison of different classifiers, in terms of accuracy (obtained through confusion matrix) when compared to ground truth map of the study area, vis-à-vis dimensionality reduction techniques.

It is clearly evident from table 4 that overall accuracy of classification is highest at 82.73% with SVM as classifier and feature extraction through image texture analysis. However, with MNF transform, maximum accuracy is yielded by Parallelpiped classifier (65%). Figure 2 shows the classified image using SVM classifier and image texture based feature extraction.

Table 4: Evaluation of classifiers for dimensionality reduction through texture analysis and MNF transform

Classification Technique	Feature extraction through Texture analysis (Overall accuracy %)	Kappa coeff.	Feature extraction through MNF transform (Overall accuracy %)	Kappa coeff.
Binary Encoding	40.9	0.203	52.6	0.323
Minimum Distance	52.2	0.335	62.7	0.484
Neural Network (Hyperbolic model)	25.3	0.129	15.5	0
Parallelpiped	55.3	0.351	65	0.55
Spectral Angle Mapper	67.9	0.484	53.5	0.35
Support Vector Machine (Linear model for activation)	**82.73**	**0.67**	64.7	0.507

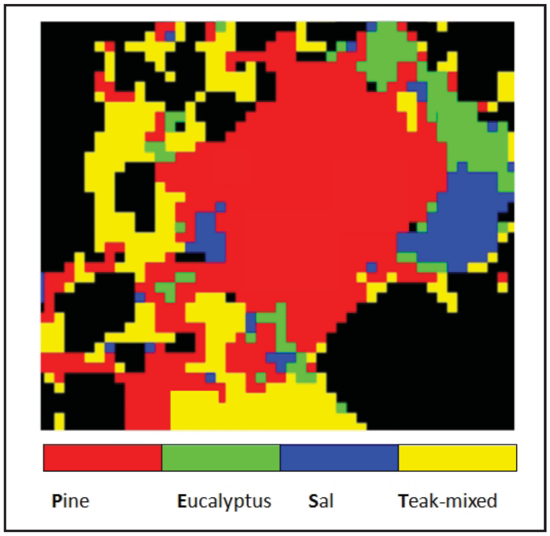

Figure 2: Classified scene of the study area using image texture based dimensionality extraction and SVM as classifier

5. Conclusion

Although, there are a number of feature extraction/reduction techniques and still greater number of classifiers for broad as well as narrow band data, one looks for the methods in terms of ease of application amalgamated with accuracy in results. In this work, image texture based feature extraction of hyperspectral data is ~~proposed~~. Conventionally popular method of feature extraction through MNF is also evaluated. Besides this, a number of classifiers are evaluated to arrive at the best combination of dimensionality reduction technique and classification method for discriminating vegetation species. Comparison of the classification output maps with the ground map yielded image texture based feature extraction clubbed with SVM classifier as the best combination. The method proposed is simple, fast and improves the classification results. However, the methods are based on one case study. Further implementation of the methods over a few more datasets in varying environments is required for ascertaining the robustness of the method for dimensionality reduction of hyperspectral images.

Acknowledgements

We are extremely grateful to Shri A.S. Kiran Kumar, Director, Space Applications Centre, ISRO, Ahmedabad for his keen interest and encouragement. We owe our sincere thanks to Dr. P. Soni from Forest Research Institute for providing us the necessary information. We are also thankful to Dr. Prakash Chauhan for his valuable suggestions.

References

Boardman, J. W., and F. A. Kruse (1994). Automated spectral analysis: a geological example using AVIRIS data, north Grapevine Mountains, Nevada: in Proceedings, ERIM Tenth Thematic Conference on Geologic Remote Sensing, Environmental Research Institute of Michigan, Ann Arbor, MI, pp. I-407 - I-418.

Champagne, C., E. Pattey, A. Bannari and I.B. Stratchan (2001). Mapping crop water status: Issues of scale in the detection of crop water stress using hyperspectral Indices. Proceedings of the 8th International Symposium on Physical Measurements and Signatures in Remote Sensing, Aussois, France. pp 79-84.

Clark, R.N., T.V.V. King, M. Klejwa and G.A. Swayze (1990). High spectral resolution spectroscopy of minerals. Journal of Geophysical Research, v. 95, no. B8, pp 12653- 12680.

Farrell, M.D. and R.M. Mersereau (2005). On the impact of PCA dimension reduction for hyperspectral detection of difficult targets. IEEE Geoscience And Remote Sensing Letters, Vol. 2, No. 2, April 2005, p. 192-195.

Green, A. A., M. Berman, P. Switzer and M.D. Craig (1988). A transformation for ordering multispectral data in terms of image quality with implications for noise removal. IEEE Transactions on Geoscience and Remote Sensing, V. 26, no. 1, p. 65-74.

Goetz, A.F.H. (2009). Three decades of hyperspectral remote sensing of the Earth: A personal view. Remote Sens. Environ., doi: 10,1016/j.res.2007.12.014.

Haralick, R.M., K. Shanmugam and I. Dinstein (1973). Textural Features for Image Classification. IEEE Transactions On Systems, Man, And Cybernetics, Vol-SMC-3, No. 6, November 1973, pp. 610–621.

Hughes, G.F. (1968). On the mean accuracy of statistical pattern recognizers. IEEE Transac. on Info. Theory, 14, 55-63.

Kruse, F.A., A.B. Lefkoff, J.B. Boardman, K.B. Heidebrecht, A.T. Shapiro, P.J. Barloon and A.F.H. Goetz (1993). The Spectral Image Processing System (SIPS) - Interactive visualization and analysis of imaging spectrometer data. Remote Sensing of the Environment, V. 44, p. 145 - 163.

Matthew, M.W., S.M. Adler-Golden, A. Berk, S.C. Richtsmeier, R.Y. Levine, L.S. Bernstein, P. K. Acharya, G.P. Anderson, G.W. Felde, M.P. Hoke, A. Ratkowski, H.-H. Burke, R.D. Kaiser and D.P. Miller (2000). Status of atmospheric correction using a MODTRAN4-based algorithm. SPIE Proceedings, Algorithms for Multispectral, Hyperspectral, and Ultraspectral Imagery VI. 4049, pp. 199-207.

Mazer, A.S., M. Martin, M. Lee and J.E. Solomon (1988). Image processing software for imaging spectrometry analysis. Remote Sensing of the Environment, V. 24, no. 1, p. 201-210.

Pearlman, J., S. Carman, C. Segal, P. Jarecke P. Barry and W. Browne (2001). Overview of the Hyperion imaging spectrometer for the NASA EO-1 mission, eo1.gsfc.nasa.gov/new/ValidationReport/Technology/19.pdf.

Richards, J.A. and Xiuping Jia (2006). Remote sensing digital image analysis. Springer-Verlag, Berlin, Germany, p. 364.

Richards, J.A. (1999). Remote sensing digital image analysis: An introduction. Springer-Verlag, Berlin, Germany, p. 240.

Schowengerdt, R.A. (1997). Remote sensing, models and methods for image processing. 2nd ed, Academic Press, San Diego, USA, 522 pp.

Shapiro, Linda G. and G.C. Stockman (2001). Computer Vision, ISBN-13: 978-0130307965 Edition: 1st

Tomita, F. and S. Tsuji (1990). Computer analysis of visual textures. Kluwer Academic Publishing, Massachusetts.